Human Molecular Genetics, 2008, Vol. 17, No. 12 ***1738–1749***
doi:10.1093/hmg/ddn064
Advance Access published on March 3, 2008

Absence seizures in C3H/HeJ and knockout mice caused by mutation of the AMPA receptor subunit *Gria4*

Barbara Beyer[1,†], Charlotte Deleuze[2,†], Verity A. Letts[1], Connie L. Mahaffey[1], Rebecca M. Boumil[1], Timothy A. Lew[2], John R. Huguenard[2] and Wayne N. Frankel[1,*]

[1]The Jackson Laboratory, 600 Main Street, Bar Harbor, ME 04609, USA and [2]Department of Neurology and Neurological Sciences, Stanford University School of Medicine, Stanford, CA 94305, USA

Received December 4, 2007; Revised and Accepted February 28, 2008

Absence epilepsy, characterized by spike–wave discharges (SWD) in the electroencephalogram, arises from aberrations within the circuitry of the cerebral cortex and thalamus that regulates awareness. The inbred mouse strain C3H/HeJ is prone to absence seizures, with a major susceptibility locus, *spkw1*, accounting for most of the phenotype. Here we find that *spkw1* is associated with a hypomorphic retroviral-like insertion mutation in the *Gria4* gene, encoding one of the four amino-3-hydroxy-5-methyl-4isoxazolepropionic acid (AMPA) receptor subunits in the brain. Consistent with this, *Gria4* knockout mice also have frequent SWD and do not complement *spkw1*. In contrast, null mutants for the related gene *Gria3* do not have SWD, and *Gria3* loss actually lowers SWD of *spkw1* homozygotes. *Gria3* and *Gria4* encode the predominant AMPA receptor subunits in the reticular thalamus, which is thought to play a central role in seizure genesis by inhibiting thalamic relay cells and promoting rebound burst firing responses. In *Gria4* mutants, synaptic excitation of inhibitory reticular thalamic neurons is enhanced, with increased duration of synaptic responses—consistent with what might be expected from reduction of the kinetically faster subunit of AMPA receptors encoded by *Gria4*. These results demonstrate for the first time an essential role for *Gria4* in the brain, and suggest that abnormal AMPA receptor-dependent synaptic activity can be involved in the network hypersynchrony that underlies absence seizures.

INTRODUCTION

Absence epilepsy is a common form of idiopathic generalized epilepsy that occurs frequently in childhood and in adolescence (1). Absence seizures are associated with spike–wave discharges (SWD) in the electroencephalogram (EEG) and are characterized by a brief loss of consciousness while the patient remains still. SWD are thought to arise from a 'perversion' of the spindle-wave activity that occurs during the early, slow-wave phases of sleep (2). This oscillatory network activity is based in cellular circuits that reciprocally connect excitatory thalamic neurons with those in the cerebral cortex. Thalamocortical and corticothalamic projections also stimulate inhibitory neurons of the thalamic reticular nucleus via axon collaterals that branch within the nucleus en route to their final targets, resulting in feedforward and feedback inhibition of thalamic neurons that is central to the rhythm generation. The reticular nucleus in particular is thought to play an essential role in SWD, as specific unilateral lesion or inactivation abolishes seizures in the ispilateral thalamocortical hemicircuit (3). Thalamocortical circuits are capable of switching modes, based on behavioral state, and thus help individuals to remain vigilant in the presence of environmental stimuli (relay state), and default to oscillatory state when at rest (2,4).

Several key ion channels are active in thalamocortical circuits that determine awareness state and are also potentially involved in the genesis of SWD. Although idiopathic general-

*To whom correspondence should be addressed. Tel: +1 2072886354; Fax: +1 2072886757; Email: wayne.frankel@jax.org
†The authors wish it to be known that, in their opinion, the first two authors should be regarded as joint First Authors.

ized epilepsies show significant heritability (5), and some gene mutations have been found in a small fraction of patients with absence epilepsy in particular (6), the genetic basis of SWD is likely to be complex. Most of what is known comes from the study of rodent models. In mouse mutants, at least two genes encoding ion channels have been causally and proximally implicated in SWD: *Hcn2*, encoding the hyperpolarization-activated cation channel, I_h (knockout mice have absence seizures and other severe neurological deficits) (7), and *Cacna1g*, encoding a low-threshold voltage-dependent Ca^{2+} channel (VDCC), where knockout mice are relatively resistant to SWD (8). Additionally, a series of SWD-prone mouse mutants harbor defects in subunits from the high-threshold VDCC family (9–12). The physiological mechanism leading to SWD in these mutants is not yet clear, although several mutants have an accompanying up-regulation of T-type Ca^{2+} channel activity (13), and in the presence of the *Cacna1g* mutation the high-threshold VDCC mutants have reduced SWD (14), suggesting a possible means of generating SWD by increasing Ca^{2+}-dependent burst firing—supported by the analysis of human mutations in T-type VDCC genes (reviewed in 6). In addition, circuit abnormalities that result from altered inhibitory synaptic responses in the reticular nucleus of *Gabrb3* mutant mice (15) are associated with abnormal thalamocortical discharge and SWD. The function or expression of other ion channels, including sodium channels, and ionotropic glutamate receptors, may be altered in other rodent models of absence epilepsy, such as the GAERS and WAG/Rij rats (16), but they are not known to be mutated in these strains, in which the SWD have a polygenic etiology (17,18) and their role in the generation of SWD is unknown. Conversely, epileptiform EEG abnormalities in common mouse strains are relatively rare.

Amino-3-hydroxy-5-methyl-4isoxazolepropionic acid (AMPA) receptors are rapidly gated ionotropic glutamate receptors that are the primary mediators of fast excitatory synaptic transmission in the CNS (19). Release of glutamate at excitatory synapses leads initially to rapid opening of AMPA receptors and membrane depolarization, which in turn promotes unblock of Mg^{2+} from *N*-methyl-D-aspartic acid (NMDA) receptors (20) and recruitment of a long-lasting synaptic excitation through the latter. Thus the strength of synaptic activation produced by AMPA receptors critically determines the composite strength of the overall synaptic response (AMPA+NMDA receptors). AMPA receptors are tetrameric assemblies of subunits GluR1–4 (also known as GluRA–D or GRIA1–4), usually heteromeric. The functional properties of synaptic AMPA receptors depend on the underlying subunit structure, which is determined by the relative expression of the four subunits as it varies in different types of neurons. GluR4 is expressed in a small number of neocortical neurons, but is known to be highly expressed in thalamus, especially in the thalamic reticular nucleus, where it is the predominant AMPA receptor at the corticothalamic synapse, showing 3- to 4-fold higher expression than at other thalamic sites (21–24). Thus defects in GluR4 function would be expected to powerfully alter corticothalamic excitability. The time course of AMPA-receptor-dependent synaptic responses are largely determined by receptor desensitization, with GluR4-containing receptors, highly expressed in thalamic reticular nucleus (21), having the fastest desensitization rate (25,26). Given the likely role of cortical output in initiating SWD (27), the corticothalamic excitation of thalamic reticular nucleus mediated by GluR4 receptors may play a key role in seizure genesis promoting the powerful excitation of thalamic reticular nucleus that can convert its output into one dominated by phasic inhibition and enhanced circuit synchrony (28,29).

The C3H/HeJ (HeJ) inbred mouse strain has been studied by mouse biologists for many years. The HeJ strain has no obvious neurological phenotype, although, as is the case with most inbred strains, it is not entirely 'normal,' and is homozygous for several detrimental mutations including retinal degeneration and susceptibility to infection (30,31). However, EEG recording revealed that HeJ exhibits a modest incidence of SWD (32–34). Furthermore, in backcrosses with the C57BL/6J (B6) mouse strain these episodes are much more prolific than in the HeJ parental strain suggesting that modifier genes regulate the incidence of SWD (32). Despite this complexity, a major allele for SWD, *spkw1*, was genetically mapped to centromeric Chromosome 9 in crosses of HeJ mice (32).

In the present study, we show that the *spkw1* allele has a mutation in *Gria4* leading to marked reduction in GluR4 protein expression, and we confirm the gene–phenotype relationship by study of *Gria4* knockout mice. We also examined knockouts for the gene encoding the other AMPA subunit expressed in the thalamus and thalamic reticular nucleus, *Gria3*, but did not observe any SWD. However, in double mutants we nevertheless find that GluR3 is required for *spkw1* mice to exhibit a high frequency SWD. Initial electrophysiological studies suggest that the effect of mutating *Gria4* is to enhance excitatory activity in the thalamic reticular nucleus by prolonging the synaptic response. We hypothesize that this enhanced activity is, in turn, critical for the network hypersynchrony associated with absence seizure.

RESULTS

The *spkw1* gene was previously defined as a major factor in SWD incidence in a cross between the C3H/HeJ substrain and wild-type C57BL/6J (B6) mice. To examine the strain specificity of *spkw1*, we analyzed backcross mice between two C3H substrains that differ in SWD incidence, HeJ and C3HeB/FeJ (FeJ). It was previously shown that both FeJ and $(HeJ \times FeJ)F_1$ hybrids exhibited relatively low SWD incidence, consistent with recessive inheritance of *spkw1* (32) (Fig. 1). However, as with the outcross to B6 described previously, the inter-C3H substrain backcross showed an approximately bimodal distribution, with mice that show very low and very high SWD incidence (Fig. 1). These surprising results show that the genetic differences affecting SWD between HeJ and B6, also exist within C3H substrains. By utilizing genetic markers to distinguish substrains, we determined that there was a highly significant association with SWD incidence, indicating that the locus of major effect maps to centromeric Chromosome 9 (Fig. 1), consistent with it being *spkw1*.

The strong effect of *spkw1* between C3H substrains prompted a closer look at candidate genes. Previously evaluated was *Gria4*, encoding the ionotropic glutamate receptor GluR4

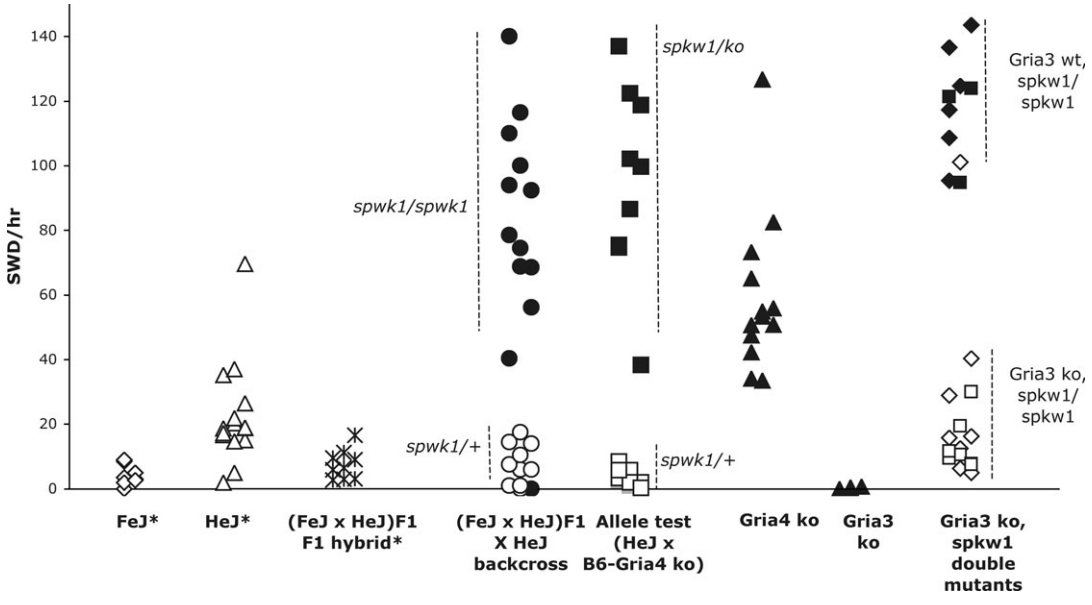

Figure 1. SWD incidence in mice with *Gria4* and *Gria3* mutations. Shown is a plot of SWD incidence, from left-to-right in FeJ, HeJ and their F1 hybrids, (*FeJ and F1 data replotted from Frankel *et al*. (32), HeJ are cumulative, including the previous data and 12 new datapoints), in intra-C3H backcross mice, in mice from the complementation test ('allele test') between HeJ (carrying *Gria4*^{spwk1}) and the B6- *Gria4* ko strain, in *Gria4* knockouts themselves, in *Gria3* knockouts and in *Gria4*^{spkw1} x *Gria3* ko double mutants. In the backcross, the allele test and in double mutants, the genotypes of mice (as determined by *D9Jmp26*—see Materials and Methods—and additional microsatellite markers) are noted by filled versus hollow points, and the groups are labeled. The arrow denotes a rare *Gria4*^{tm1Dgen} homozygote from the backcross that is SWD-resistant, presumably due to modifier loci (see text). At the far right, for double mutants, diamonds denote N_2 generation and squares N_4 generation. Littermate controls for the knockout mice did not show any SWD (not shown). Each point represents the average number of SWD for an individual mouse, from at least 4 h of recording on two separate days. Representative EEG traces from each genotype that displays SWD are shown in Supplementary Material, Figure S1.

(also known as GLUR4 and GluR-D, the official protein symbol is now GRIA4), but neither coding sequence nor major gene expression differences were observed between HeJ and wild-type strains, provisionally excluding its candidacy (32). However, during the course of genome-wide microarray experiments, two probe sets from the 3′ end of the *Gria4* gene showed significant differences in gene expression between FeJ, HeJ and high-SWD backcross mice (Supplementary Material, Table S1). The location of the probe sets and nature of the expression difference prompted us to look in the last few introns of *Gria4* for mutations that might affect gene expression in HeJ mice. Genomic PCR and sequencing revealed a full-length intracisternal A-particle (IAP) proviral insertion in the last intron, present in HeJ but absent from B6 and FeJ strains (Fig. 2, Supplementary Material, Fig. S1). IAP insertions are well-known spontaneous mutations in C3H mouse strains (35). Although the specific mechanism of mutagenesis may vary, IAP's are generally thought to interfere with RNA splicing, read-through RNA transcription or both, wherever the affected gene is expressed (35). Quantitative RT–PCR showed an approximately 10-fold difference between HeJ and FeJ substrains in the amount of transcript detected between exons flanking the IAP-containing intron, compared with a negligible difference between upstream exons—consistent with an effect of the IAP on splicing or transcriptional readthrough (Fig. 3A). Furthermore, decrease in transcript levels was accompanied by a significant reduction in the amount of GluR4 protein in HeJ cerebellum compared with control (Fig. 3C)—suggesting that HeJ carries a severely hypomorphic allele of *Gria4*.

To confirm the causal relationship between *Gria4* deficiency and SWD, we assessed the electroencephalographic phenotype of an independent mutation of *Gria4*: the *Gria4*^{tm1Dgen} knockout allele (expression defect data are shown in Figure 3B and C; see Materials and Methods for more details on the origin and nature of *Gria4*^{tm1Dgen}). First, we determined whether or not *Gria4*^{tm1Dgen} could functionally complement the *Gria4*^{spkw1} allele by comparing SWD incidence in compound heterozygotes (*Gria4*$^{spkw1/tm1Dgen}$) with that of controls (*Gria4*$^{spkw1/+}$); failure of linked recessive mutations to complement each other usually suggests that the phenotype-causing mutations reside in the same gene. All of the compound heterozygotes had a very high SWD incidence, about 90 SWD/h, compared with the *Gria4*$^{spkw1/+}$ mice (Fig. 1, allele test), suggesting allelism. We then examined homozygous B6-*Gria4*^{tm1Dgen} mutants themselves and observed a high incidence of SWD (Fig. 1, *Gria4* ko), revealing clusters of EEG spike and wave events with similar characteristics to those of HeJ backcross mice (Fig. 4A). Although the incidence was not as high as in some compound heterozygotes or in *Gria4*^{spkw1} homozygous backcross mice, we suspect that genetic background (in this case, homozygosity for modifier alleles from B6) contributes to the phenotype. As shown for the *Gria4*^{spkw1} allele previously, the SWD of homozygous *Gria4*^{tm1Dgen} mice coincide with an arrest of normal behavior and are suppressed by treatment with the anti-absence drug ethosuximide (Fig. 4B). Together these data show that a genetic deficiency in *Gria4*, whether reduction (*Gria4*^{spkw1} allele) or complete lack (*Gria4*^{tm1Dgen} allele), is associated with a high frequency of SWD, modeling absence epilepsy.

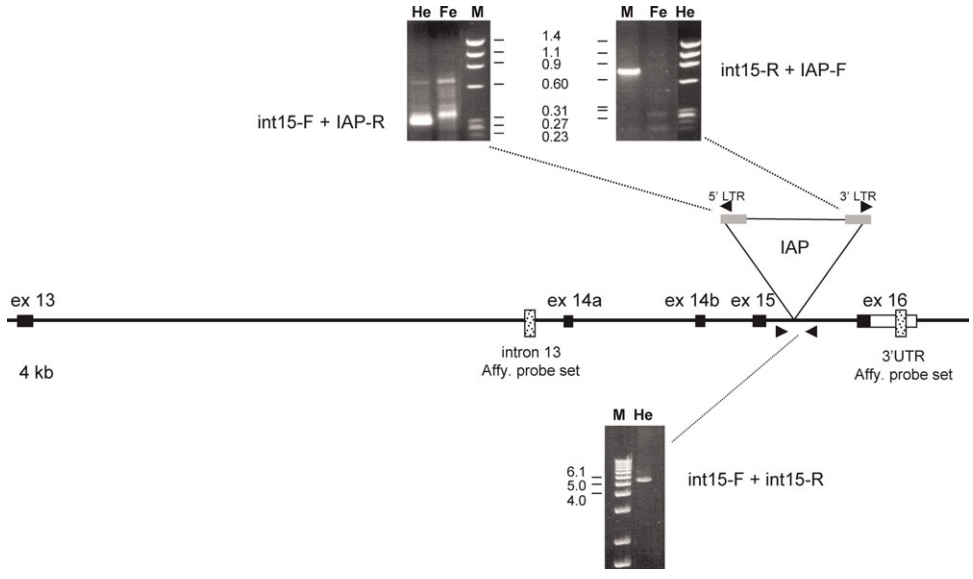

Figure 2. C3H/HeJ mice have an IAP insertion in the last intron of *Gria4*. Shown is a map of the 3′ end of the *Gria4* gene, from exon 13 to exon 16, noting the location of the IAP proviral insertion, with 5′ and 3′ long terminal repeats. Also shown are the locations of primers used to amplify the proviral-*Gria4* junction fragments, as well as the entire provirus. Images of the respective amplification products are also shown from HeJ (He) and FeJ (Fe) mice, described in Materials and Methods, along with DNA markers (M, HaeIII digested bacteriophage PhiX DNA, or a ladder). Probe sets giving significant gene expression differences (see Supplementary Material, Table S1) are shown as stippled boxes.

Gria3 encodes GluR3, the other predominant AMPA receptor expressed in the thalamocortical network. To gain insight into the possible role of GluR3 in SWD, we characterized the EEG of mice that lack GluR3, *Gria3*^{tm1Dgen} (obtained from the same source as *Gria4* knockouts– see Materials and Methods). Mice that lack GluR3 show no SWD (Fig. 1, *Gria3* ko). However, double mutant mice show a much lower incidence of SWD than do *Gria4*^{spkw1} homozygotes alone (Fig. 1; *Gria3* ko, *spwk1* double mutants); this result, observed in the first backcross, or N_2 generation, was also confirmed in the N_4 generation (Fig. 1) supportive of the primacy of the *Gria3*–*Gria4* genetic interaction. These data show that the presence of GluR3 is required to observe the high SWD incidence phenotype conferred by homozygosity of *spkw1*. Interestingly, while double mutant mice appear outwardly normal as young adults, after ∼3 months of age they develop a mild-to-moderate cerebellar ataxia, compared with their single mutant littermates, suggestive of the functional importance of normal levels of GluR3 and GluR4 together in the cerebellum, where both are expressed at high levels.

AMPA receptors are strong candidates for regulating the generation and propagation of SWD because they provide the major basis for cortical excitation of thalamic reticular nucleus cells (2,4). GluR4, in particular, is the predominant AMPA receptor expressed in the thalamic reticular nucleus, where it is expressed 3- to 4-fold higher at corticothalamic synapses than at other reticular and intrathalamic sites, making the thalamic reticular nucleus a potentially critical site of action; GluR3 is also expressed but at lower levels (21,36).

To initially determine whether the *Gria4*^{spkw1} mutation affected the synaptic activity of reticular thalamus inhibitory neurons, we examined spontaneous excitatory postsynaptic currents (sEPSCs, see Materials and Methods) of *Gria4*^{spkw1} homozygous intra-C3H backcross mice with very high incidence of SWD and of heterozygous littermate control mice. These experiments were done in the presence of D-CPPene to block NMDA-receptor-mediated portion of the synaptic responses, thus isolating the AMPA receptor component. In *Gria4* ^{spkw1} homozygous mice, sEPSCs had reduced amplitudes (39.4 ± 0.3 pA) and longer durations (half width: 0.47 ± 0.003 ms; $n = 5882$ sEPSCs in nine cells) compared with littermate controls (54.4 ± 0.3 pA, 0.36 ± 0.002 ms; $n =$ 9032 sEPSCs in 12 cells; $P < 0.01$; Fig. 5). This overall effect is especially due to a decrease in the number of brief, large-amplitude events (Fig. 5C1–C3), consistent with altered GluR4 receptor expression. Although the overall synaptic charge was slightly increased in mutant neurons, the changes are not statistically significant (Fig. 5C3, inset). As GluR4 containing AMPA receptors express fast decay kinetics, e.g. compared with the other subunit expressed in the reticular thalamus, GluR3 (22,23), then loss of GluR4 would be expected to increase the duration of the excitatory synaptic responses, consistent with our observations. Presumably while GluR3 may be compensating, perhaps through an increased synaptic expression to restore quantal synaptic charge to control levels, the putative GluR3 compensation is ultimately unable to replace the essential function of GluR4, perhaps due to the difference in decay kinetics. We did not observe any gross difference in GluR3 expression in either *spwk1* or in *Gria4* null mice, in the cerebral cortex or in microdissected thalamus/reticular thalamus (Supplementary Material, Fig. S4).

DISCUSSION

The C3H/HeJ (HeJ) strain and mice derived from it have significant SWD accompanied with behavioral arrest, characteristic of absence epilepsy. This phenotype, caused by

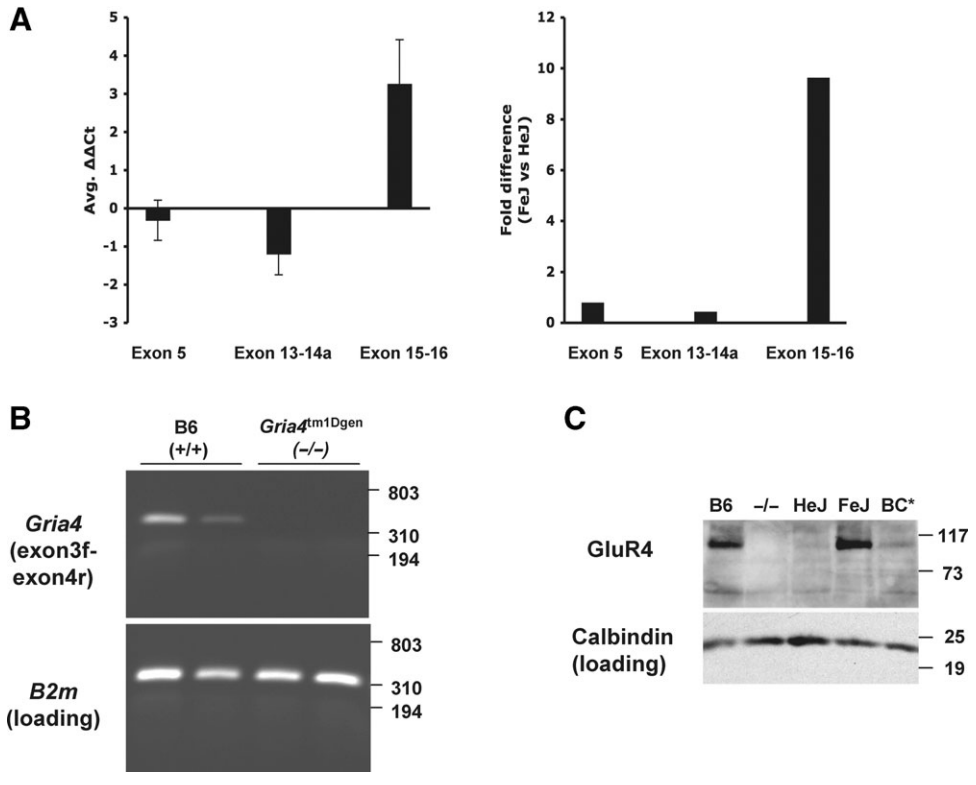

Figure 3. Decreased GluR4 gene and protein expression in *Gria4* mutant mice. (**A**) Differential expression of *Gria4* transcript in FeJ versus HeJ mice. Shown are ΔΔCt values (left, ± 1SD) and approximate fold-difference ratios (right) for three different regions of the *Gria4* transcript, as indicated, in cDNA prepared from adult mouse whole brain. The amount of *Gria4* transcript spanning exons 15–16 is almost 10-fold lower in HeJ mice, which harbor the IAP insertion in intron 15, than in FeJ mice. (**B**) *Gria4* transcripts from exon 3 to exon 4 are undetectable in $Gria4^{tm1Dgen}$ homozygotes. Shown is conventional RT–PCR from exon 3 to 4 in $Gria4^{tm1Dgen}$ (knockout) mice versus B6 (+/+) controls, where no transcript was detected in duplicate samples. *B2 m* gene transcript served as a positive control for all samples. (**C**) Representative (of three trials) western blot analysis of GluR4 expression in cerebellar preps from B6, $Gria4^{tm1Dgen}$, C3H/HeJ, C3H/FeJ and BC* ($Gria4^{spwk1}$ homozygous backcross) adult mice. Below, the calbindin level is shown as the loading control for this blot. GluR4 protein is decreased in HeJ and BC* mice, and absent from $Gria4^{tm1Dgen}$ homozygotes. Although cerebellum is not involved in epilepsy, here it is used as a genetic control since GluR4 is expressed very highly in this region and the antibody is not of sufficient quality to detect protein from thalamus on western blots.

retroelement insertion in intron 15 of the gene encoding GluR4 (*Gria4*), disrupting gene expression, represents the first naturally occuring functional variant of the *Gria4* gene. Both RNA and protein analyses confirm that full-length *Gria4* expression is significantly reduced in this strain. The causal effect on phenotype was further confirmed in a gene-targeted allele of *Gria4* that does not complement the *spkw1* mutation of HeJ and independently shows frequent SWD. In double mutant studies, we also determined that while loss of *Gria3* alone does not result in SWD, its presence is nevertheless associated with the high incidence of SWD in mice homozygous for the $Gria4^{spkw1}$ allele. Further, while C3H/HeJ mice do not exhibit locomotor impairment, some C57BL/6J mice homozygous for the $Gria4^{tm1Dgen}$ knockout allele develop a mild cerebellar ataxia and all $Gria4^{spkw1}$, $Gria3^{tm1Dgen}$ double mutants develop mild-to-moderate ataxia after 3 months of age. These results suggest that *Gria4* deficient mice are very close to the threshold for abnormal cerebellar function, whereby certain background genotypes can cause *Gria4* mutant mice to experience locomotor impairment.

Gria4 encodes one of four AMPA receptor subunits that form the tetrameric functional receptor complex (37). Although both *Gria3* and *Gria4* expressed in the reticular thalamus, it has been shown previously that *Gria4* encodes the predominant subunit in this critical region which, together with the cortex and thalamus form the thalamocortical circuit (4). Perturbations altering the balance of excitation and inhibition within this circuit are believed to underlie awareness and absence epilepsy (2,38). The reticular nucleus appears to play a major role in SWD generation, as either temporary or excitotoxic lesions of the nucleus result in blockade of SWD in the well-characterized GAERS model (3), and local infusion of agonists and antagonists of inhibitory GABA receptors leads to exacerbation or blockade of the seizures, respectively (39,40). Furthermore, the GRIA4-enriched AMPA receptor has been shown to exhibit a rapid response to glutamate (26). Thus, in mice with greatly reduced *Gria4* expression, the AMPA receptor composition would change in the reticular thalamus, resulting in the observed changes to AMPA receptor function. Further, the increased duration of excitatory input of thalamic reticular neurons in the C3H/HeJ strain would likely lead to an increased efficacy of corticoreticular (and also thalamoreticular) synapses, especially during repetitive activity, which would, in turn, promote powerful burst firing in reticular neurons. Indeed, in preliminary studies we observe a significant prolongation of the excitatory synaptic response after repetitive stimulation of corticothalamic/thalamocortical fibers, supporting this hypothesis (C. Deleuze and J. Huguenard, unpublished results).

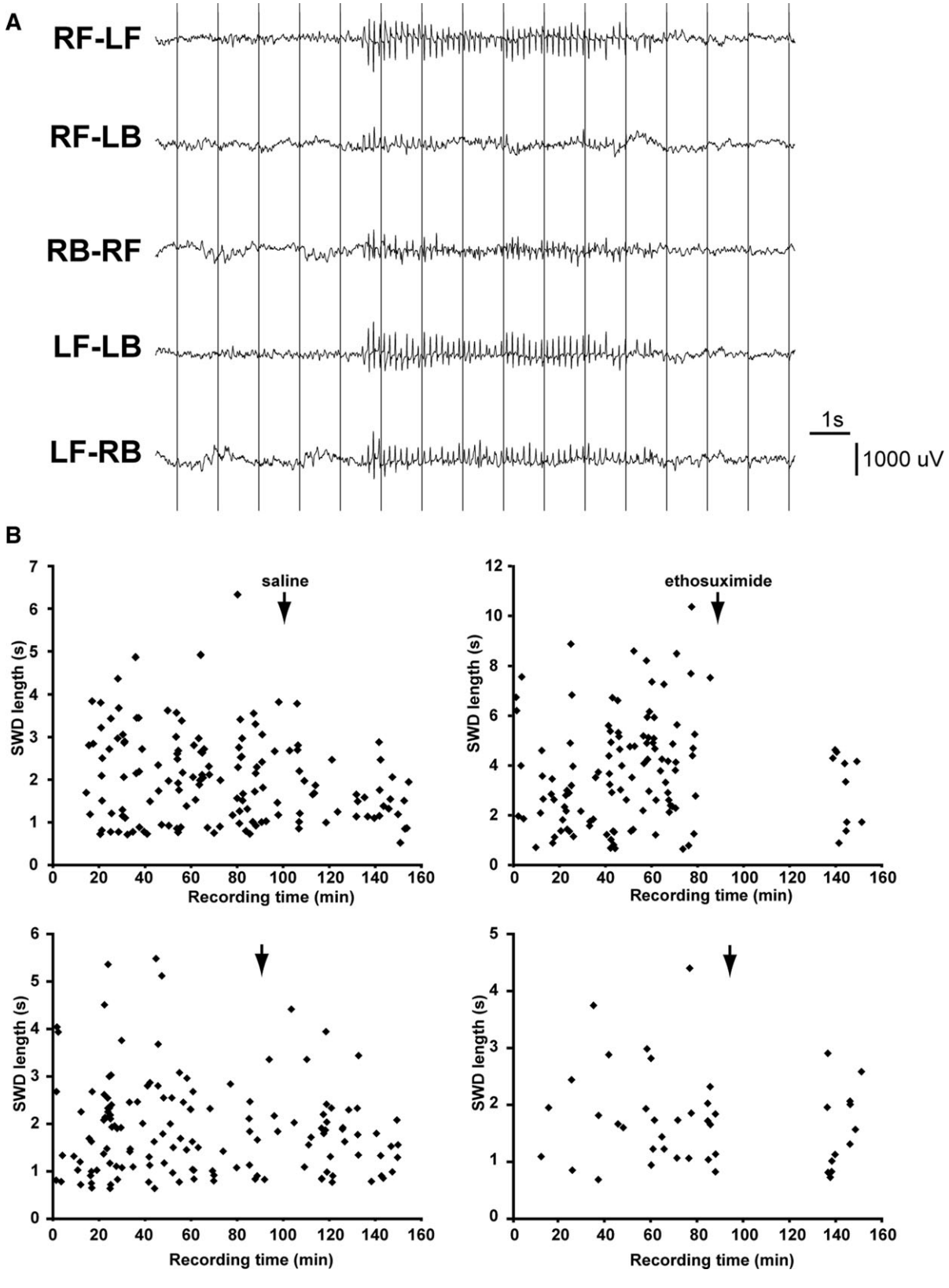

Figure 4. SWDs in *Gria4*^{tm1Dgen} mice. (**A**) Representative EEG of a *Gria4*^{tm1Dgen} homozygous mouse, showing the six differential traces from the four electrodes, over the right front (RF), left front (LF), right back (RB), left back (LB) surfaces of the cerebral cortex, and a representative spike–wave burst lasting ~6 s with its characteristic high amplitude, synchronous, rhythmic and generalized pattern. (**B**) Plots of SWD length and incidence in a typical recording session of four different *Gria4*^{tm1Dgen} homozygous mice, treated with either 200 mg/kg ethosuximide (ETX—right side), or normal saline (left), injected subcutaneously after ~90 min of recording (arrows). Note the cessation of SWD for 50 min post-injection, seen only in the ETX-treated mice, followed by SWD activity.

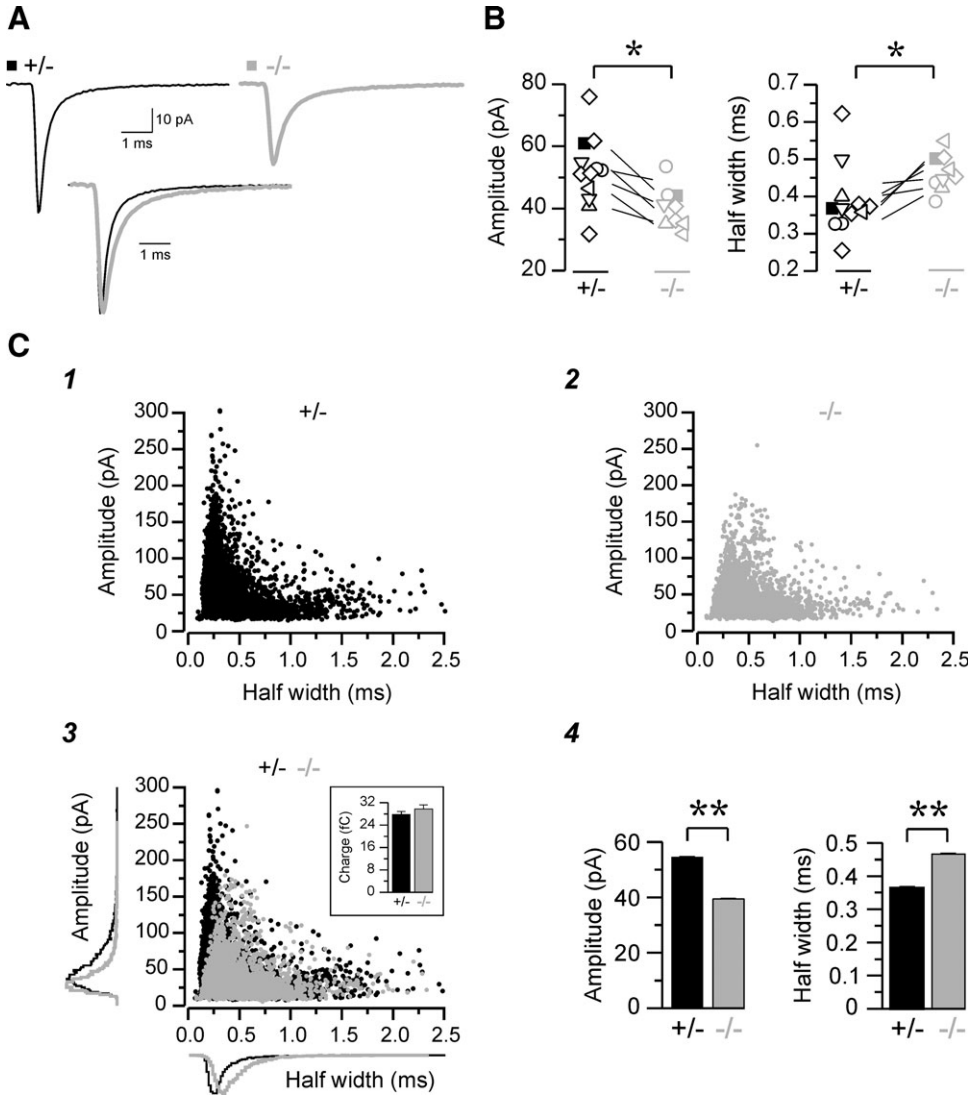

Figure 5. Spontaneous synaptic activity of the thalamic reticular nucleus in homozygous versus heterozygous *Gria4*^{spwk1} mice. (**A**) Spontaneous EPSCs recorded in two cells from littermate heterozygous (+/−, black) and homozygous (−/−, gray) mice. Each trace represents the average of all well-isolated individual EPSCs per cell and are plotted either separately (top panels) or normalized to the peak and overlaid (bottom). (**B**) Scatter representation of the mean amplitude and half width of spontaneous EPSCs recorded from individual +/− ($n = 12$) and −/− ($n = 9$) cells, each represented by a single symbol. Each type of symbol (e.g. ○,◇,□.) indicates cells belonging to the same pair of littermate +/− and −/− mice (six pairs total). Each diagonal line is the comparison between the mean responses measured for each littermate pair. One pair was examined on each experimental day. The experimenter was blinded as to mouse genotype during recording and analysis. The filled symbols correspond to the +/− and −/− littermate cells shown in (A). The overall population of cells shows significantly smaller and slower EPSCs in homozygous mice. (**C**) Total population of EPSCs recorded in +/− (black, $n = 9032$ events in 12 cells) versus −/− (gray, $n = 5882$ events in nine cells) mice. The scatter plots illustrate the relationship between half width and amplitude of EPSCs in +/− (*C1*) and −/− (*C2*) mice, each point representing an individual event. In panel C3, the data from C1 (+/−, black) and C2 (−/−, gray) are also shown overlapped on a single graph, together with the normalized distribution of the same parameters plotted outside the X and Y axes. Note the lack of large and fast events in −/− neurons. Plotted on *C4*, the corresponding histograms show a significant decrease in amplitude and increase in duration in mutants, whereas the mean synaptic charge per EPSC was slightly increased, but the changes are not significantly different (inset). $^{*}P < 0.05$; $^{**}P < 0.01$.

We expect that increased excitation in the thalamic reticular nucleus increases the ability of the thalamocortical circuit to activate the reticular neurons, thus producing the powerful inhibitory drive necessary for SWD generation. Computational modeling suggests that synaptic integration in the reticular nucleus depends critically on the relative durations of excitatory versus inhibitory synaptic currents (41). Brief excitatory synaptic response can be shunted by a concurrent inhibitory response whose duration outlasts the excitatory response, while longer lasting responses are less effectively shunted. Thus in the mutants the dynamic balance between excitation and inhibition within the reticular nucleus would be altered in favor of the former. This would result in enhanced feedforward inhibition from reticular neurons to thalamic relay neurons and robust rebound burst responses that strongly reinforce the larger thalamocortical network oscillation. The model is consistent with studies in rats showing that increased cortical activity is associated with early seizure stages and this

is followed by later thalamic recruitment and widespread epileptic activity (27,42). The ability of repetitive cortical feedback to strongly recruit reticular neuron firing in brain slices is also consistent with this scheme (28,29). However, the model we favor for SWD in *Gria4* mutant mice is still preliminary, with several caveats; for example, the relative contributions of altered corticothalamic versus thalamocortical excitatory inputs to the reticular nucleus are not yet known. In addition, loss of *Gria4* during development may have led to compensatory mechanisms. More detailed physiological studies are required to examine these possibilities.

The association of *Gria4* deficiency with a high rate of SWD is also interesting in view of stargazer mice, which have a similar epileptic phenotype along with other neurological impairments (43,44). The stargazin protein was initially proposed to be the neuronal γ subunit for the P/Q-type (i.e. $Ca_v2.1$) VDCC, based on its evolutionary relationship to the γ1 subunit of the L-type channel in cardiac tissue, electrophysiological characteristics similar to that of γ1 (12) and the fact that three other mouse mutants with mutations in the more conventional subunits of the P/Q-type Ca^{2+} channel also have SWD (9,44–46). But it has more recently been shown that stargazin is responsible for AMPA receptor trafficking and gating (47,48). Future studies are needed to explore whether there are similarities between the pathophysiology of *Gria4* deficient mice, e.g. sustained excitation of the reticular thalamic nucleus, and that of stargazer mice.

Gria4 mutants on the C3H strain confer a range of phenotypic effects that are dependent upon genetic background. The striking increase of SWD in $Gria4^{spkw1}$ homozygous backcross mice compared with $Gria4^{spkw1}$ homozygous HeJ parents (∼100 SWD/h versus ∼20 SWD/h, respectively; Fig. 1) implies that HeJ has genetic modifiers which actually mitigate thalamocortical hypersynchrony; the low incidence of SWD-resistant $Gria4^{spkw1}$ homozygotes in backcross mice (e.g. arrow in Fig. 1), is consistent with several modifier loci. The modifiers may not only affect SWD quantitatively but also their timing with respect to arousal state. That is, while backcross mice usually exhibit SWD from the onset of a recording session [(32), similar to $Gria4^{tm1Dgen}$ in Fig. 4B], HeJ mice have a lag of at least 20–30 min before their first SWD, which usually appear when the animals cease exploring their new environment and begin settling-in to their nests (32). This is interesting in view of the prevailing view that absence seizures are fundamentally a perversion of the normal thalamocortical circuitry that regulates behavioral awareness (2). Although further work is necessary to characterize the modifiers, the spectrum of SWD phenotypes seen in C3H strains—from the very low (FeJ) to modest (HeJ) to high (backcross) SWD incidence—provide a new opportunity to understand and study the regulation of thalamocortical synchrony and relationship to arousal state.

There is considerable literature showing that AMPA receptors are important for synaptic plasticity (49). We now provide the first genetic and physiological evidence that they are critical for normal thalamocortical function *in vivo*, in particular by demonstrating that altering the delicate balance between AMPA receptor subunits in mice can lead to absence epilepsy.

MATERIALS AND METHODS

Mice

All mice were housed and bred with approval of Institutional Animal Care and Use Committee (IACUC). C3H/HeJ, C3HeB/FeJ and C57BL/6J mice were obtained from The Jackson Laboratory. $Gria4^{tm1Dgen}$ knockout mice were developed and initially characterized by Deltagen (see http://www.informatics.jax.org/external/ko/deltagen/1624.html) and made available via the NIH-funded Mouse Mutant Regional Resource Center (MMRRC; http://www.mmrrc.org), in particular, the node at University of North Carolina, for a $1100 fee and Material Transfer Agreement. Forty-nine frozen embryos from a mating between a heterozygote and a C57BL/6J mouse were shipped to the Assisted Reproduction service at The Jackson Laboratory and implanted into the uterus of suitable recipient females. Three embryos survived to term, all of which were heterozygous for the $Gria4^{tm1Dgen}$ allele. These mice were subsequently mated to each other or to C3H/HeJ to generate homozygotes and compound heterozygotes, respectively. During the course of genotyping for homozygosity, however, we discovered that the $Gria4^{tm1Dgen}$ allele did not harbor the reported homologous replacement of *Gria4* exon 3 with the lacZ-neo cassette, leaving a truncated exon 3. Instead, long-PCR and genomic sequencing revealed that the 5' half of the [*Gria4* intron 3 arm—lacZ-neo cassette—*Gria4* intron 3 arm] construct inserted into the *Gria4* intron 3, resulting in a truncation of most of the lacZ gene, and some of intron 3 as well (although a 2.8 kb duplication of the part of intron 3 adjacent to exon 3 also occurred; Supplementary Material, Fig. S2). We presume that some of the 3′ arm of the construct inserted homologously. Although this resulted in an intact native exon 3, no brain RNA was detected by using exon 2–exon 4 (data not shown), or from exon 3–exon 4 primers by RT–PCR (Fig. 3A). This, plus the absence of protein on western blot from homozygous mutants (Fig. 3B), suggests that despite the abnormal targeting event, the $Gria4^{tm1Dgen}$ allele is nevertheless null. $Gria3^{tmDgen}$ mice were also imported from the same source; our mice were hysterectomy derived from the progeny of a single heterozygous female, mated to wild-type C57BL/6J mice. Unlike the case with $Gria4^{tm1Dgen}$, we find that the molecular lesion in *Gria3* is exactly as described by Deltagen (see http://www.informatics.jax.org/external/ko/deltagen/1623.html), i.e. the target exon 11 replaced with a LacZ fusion protein). Although *Gria3* null mutants do not show any overt neurological phenotype, a fraction (<10%) of *Gria4* null mutants on the C57BL/6J background do exhibit a mild cerebellar ataxia, which becomes more pronounced with age. Nevertheless, the majority of *Gria4* null mutants on the C57BL/6J background do not develop ataxia.

EEG analysis

Mice were anesthetized with tribromoethanol (400 mg/kg i.p.) Small burr holes were drilled (1 mm anterior to the bregma and 2 mm posterior to the bregma) on both sides of the skull 2 mm lateral to the midline. EEG activity was measured by four Teflon-coated silver wires soldered onto a microconnector. The wires were placed between the dura and the brain and a dental cap was then applied. The mice were given a

post-operative analgesic of carprofen (5 mg/kg subcutaneous) and were given a 48 h recovery period before recordings were made. The mice were recorded for a 2-h period on each of the following 2 days using the Grass EEG Model 12 Neurodata Acquisition System and PolyViewPro software program (Grass-Telefactor, Inc.) or Stellate Harmonie (Stellate, Inc.). For *Gria4*^{tm1Dgen} homozygous mice that were treated with ethosuximide, on the day following their second standard EEG recording, mice were recorded for 90 min and then injected interperitoneally with 200 mg/kg ethosuximide (Sigma-Aldrich, Inc.), as shown in Figure 4B. They were then recorded for a minimum of one additional hour. The control mice were injected interperitoneally with saline and recorded in the same manner. All mice were used with approval of IACUC.

Genotyping

Linkage of the SWD phenotype in intra-C3H backcross shown in Figure 1 was done using the microsatellite marker at 6.2 Mb on Chromosome 9, *D9Jmp26* (F primer: 5′-GTGATGC CATGTCCATGATT-3′; R primer 5′-ATGGGCAAGTAC ACCTCCAC-3′). The *Gria4*^{spkw1} allele (IAP insertion in *Gria4* intron 15 of C3H/HeJ mice) was genotyped in standard PCR conditions and agarose gel electrophoresis using one assay for the wild-type allele (primers G4-4334-F 5′-TCC AACCCATAATAAGGACTGC-3′; G4-4334-R 5′-GTGAG TGAACTGAGGGCTTA-3′), and either of two assays for the insertion allele using IAP long terminal repeat primers (JS140alt 5′-AAGATTCTGGTCTGTGGTGTTCT-3′; JS139 5′-CTGTGTTCTAAGTGGTAAAC-3′ to the respective G4-4334 primer, above).

The *Gria4*^{tm1Dgen} mutation (Deltagen knockout) was genotyped in standard PCR conditions as above by using simple sequence repeat markers flanking the *Gria4* gene on Chromosome 9, distinguishing 129 strain and B6 strain polymorphisms in the incipient B6.129-*Gria4* congenic strain in 2% agarose gels. The centromeric marker was *D9Jmp106*: forward: 5′- CTTTCTTGCCCCCTTCATTA-3′; reverse: 5′-CCAGTCACAAACACATGGACA-3′) giving product sizes of 117 bp (129 or ko allele) versus 129 bp (C57BL/6J or wt allele). The telomeric marker was *D9Jmp132* (forward 5′-CGGTCCAATTAGTTCGGTTT-3′; reverse: 5′-GATGGG ACTCGGCTATTGAA-3′), giving product sizes of 133 bp (129 or ko allele) versus 151 bp (C57BL/6J or wt allele). The mutant allele could also be amplified using Gria4Rdgen primer: 5′ TGTCACAGCAAAACTGTTGGCAGTC-3′ and NeoF: 5′-GGGTGGGATTAGATAAATGCCTGCTC-3′, but this assay only distinguishes wild-type from heterozygous mice.

The *Gria3*^{tm1Dgen} mutation was genotyped in standard PCR conditions as above in a 3-primer assays using oligonucleotides designed by Deltagen 39637: 5′- GGTCACGAGGTTCTT CATTGTTGTC-3′, 3196 (neo): 5′- GGGTGGGATTAG ATAAATGCCTGCTCT-3′, and 39636: 5′- AGCTGATATAG CTGTTGCTCCACTC-3′, giving a 380 bp product for the targeted allele and a 275 bp product for the endogenous allele.

Long-range PCR

The IAP insertion in Gria4 intron 15 was amplified using primers G4-4334-F and G4-4334-R (above) and Expand Tm DNA polymerase (Perkin-Elmer Cetus). The LacZ-neo cassette, as well as the Gria4–5′ arm targeting construct junction was amplified in the same manner using primers Gria45′armFalt (5′-GGATGGATTGTTGAGGGAAA-3′) and neo7019R (5′-GCTCCAATCCTTCCATTCAA-3′), or 32972 (5′-CCACCTCCAGAGCCGGTTCCTCGGC-3′), and LacZR-5 (5′-GGAGGAGTAGAATGTTGAGAGTC-3′), respectively. Fragments were purified using a Qiagen kit and submitted to The Jackson Laboratory DNA sequencing service.

Real-time reverse-transcription PCR

Total RNA was prepared from the whole brain of adult C3H/HeJ and C3HeB/FeJ mice with Trizol (Invitrogen) and treated with DNase I (Promega) under the manufacturer's suggested conditions. RNA (2 μg) was reverse transcribed with AMV reverse transcriptase (Promega). The cDNA was diluted 20-fold, and 1.5 μl was added to qPCR Mastermix Plus for SYBR Green I (Eurogentec) with pairs of the following primers; *beta-actin*F (5′- CATTGCTGACAGGATGCAG AA-3′) and *beta-actin*R (5′- GCCACCGATCCACACAGAG T-3′), *Gria4*exon5F (5′- CTGCCAACAGTTTTGCTGTG A-3′) and *Gria4*exon5R (5′- AGCACTGCAGAAGGAGGT CAA-3′), *Gria4*exon15F (5′- AGGGCAGAGGCGAAGA GAAT-3′) and *Gria4*exon16R (5′- TTCTGTCCGGCACTC AGGATGT-3′), *Gria4*exon13F (5′- CCAAAGGCTATGGTG TAGCGA-3′) and *Gria4*exon14aR (5′- TGCCACATTCTCC TTTGTCGTA-3′). The PCR reactions were analyzed on an ABI Prism 7000 Sequence Detection System (Perkin Elmer). The PCR amplifications from two pairs of age-matched males were run in triplicate. Amplification of the correct size products was confirmed by agarose gel electrophoresis.

Microarray analysis

Three 3.5 month females each of C3HeB/FeJ, C3H/HeJ and (C3H/HeJ × C3HeB/FeJ)F1 × C3H/HeJ (backcross mice) were used for gene expression analysis. The backcross mice had undergone EEG analysis to confirm high incidence SWD phenotype. Mice were euthanized by cervical dislocation. Immediately following death, brain tissue was extracted. The cerebellum, olfactory bulbs and all brain tissue from the right side were separated and snap-frozen in liquid nitrogen. The right cortex and remaining parts of the right brain, herein called the midbrain–hindbrain, were isolated from each other for RNA extraction, cDNA preparation and Affymetrix microarray processing—done in The Jackson Laboratory Gene Expression service. Ten micrograms of total RNA was prepared to generate 15 μg cRNA for hybridization to the Affymetrix 430 v2.0 Gene Chip (Affymetrix) according to manufacturer's recommendation. Using the R/maanova package (50), an analysis of variance model was applied to the data, and F1, F2, F3 and Fs test statistics were constructed along with their permutation *P*-values.Two microarrays were done on each mouse; one using cDNA isolated from right cortex tissue RNA, the other using the right midbrain–hindbrain cDNA isolate. Three replicate arrays were done for each substrain, generating 18 arrays. Pairwise comparisons analyses were completed, with gene expression levels used to generate fold-change values, initially between backcross and

FeJ, and then between HeJ and FeJ, and for each tissue type, resulting in four different comparisons.

Western blots

Cerebellum, thalamus (including reticular thalamus) and cerebral cortex from adult mice were dissected, homogenized and suspended on ice in lysis buffer (150 mM NaCl, 20 mM Tris–Cl, 2 mM EDTA, 1% Triton X-100, 0.05% SDS, 1 mM PMSF, pH8) with Complete Protease Inhibitor Cocktail (Roche, IN). Tissue homogenates were centrifuged at 10 000 rpm for 10 min at 4°C. The supernatants were retained and frozen at −20 C. Protein concentration was estimated using the Bradford Reagent (Sigma-Aldrich, MO). Total proteins (10–20 μg) were resolved on 8–16% Tris–Glycine PAGE gels (Cambrex Bio Science, ME). The gels were electroblotted with Protran BA83 nitrocellulose membrane (Whatman Schliecher & Schuell, NJ). Membranes were blocked with TBST (140 mM NaCl, 10 mM Tris, 0.05% Tween 20, pH7.5) with 5% evaporated milk at 23°C for 30 min, washed and then incubated in primary antibody in TBST for 1 h at 23°C. Rabbit polyclonal antibody dilutions were as follows: 1:200 for GluR3 or GluR4 carboxy terminus (Chemicon, CA); 1:5000 for Calbindin D-28 k (Swant, Switzerland); 1:1000 for β-tubulin (Sigma-Aldrich, MO). Blots were washed in TBST and incubated in TBST with 5% milk containing 1:10 000 horseradish peroxidase-conjugated secondary antibody (PerkinElmer, MA) for 1 h at 23°C. Protein bands were detected using the ECL-plus chemiluminescent reagent (Amersham Biosciences, NJ).

In vitro slice preparation

All experiments were carried out according to protocols approved by the Stanford Institutional Animal Care and Use Committee. During each experiment, a *Gria4*$^{spkw1/+}$/*Gria4*$^{spkw1/spkw1}$ pair of (FeJ × HeJ)F1 × HeJ backcross mice (∼1 month old) were anesthetized with pentobarbital (50 mg/kg), decapitated and the brains rapidly removed and immersed in an ice-cold (4°C) slicing solution containing (in mM): 234 sucrose, 2.5 KCl, 1.25 NaH2PO4, 10 MgSO4, 0.5 CaCl2, 26 NaHCO3 and 11 glucose; equilibrated with 95% O_2 and 5% CO_2; pH 7.4. Horizontal thalamic slices (250 μm) containing the reticular nucleus as well as both corticothalamic and thalamocortical tracts were cut and incubated in artificial cerebrospinal fluid containing (in mM): 126 NaCl, 2.5 KCl, 1.25 NaH_2PO_4, 1 $MgCl_2$, 2 $CaCl_2$, 26 $NaHCO_3$ and 10 glucose; equilibrated with 95% O_2 and 5% CO_2; pH 7.4, initially at 32°C for 1 h, and subsequently at room temperature, before being transferred to a recording chamber.

Patch clamp recordings

Thalamic reticular neurons were visually identified using infrared video microscopy. In addition, the identity of the cells was confirmed based on electrophysiological criteria related to the action potential firing of thalamic reticular nucleus cells (recorded in current clamp mode). Recordings were performed at 32°C in the whole-cell configuration. Electrodes (tip resistance of 2–3 MΩ) were filled with the internal solution containing (in mM): 120 K-gluconate, 11 KCl, 1 $CaCl_2$, 1 $MgCl_2$ 10 HEPES, 11 EGTA pH 7.3 adjusted with KOH; 290 mOsm. Under these recording conditions, in voltage clamp mode, activation of glutamate receptors resulted in inward currents at a holding potential of −70 mV. AMPA-receptor-mediated EPSCs were isolated in 50 μM picrotoxin (Tocris), a $GABA_A$ receptor blocker and 10 μM 3-[(R)-2-carboxypiperazin-4-yl]-prop-2-enyl-1-phosphonic acid (D-CPPene, Tocris), an NMDA receptor antagonist, both added to the bath. The access resistance was always <15 MΩ and constantly monitored for stability, and data from cells showing changes >25% of the initial value were rejected.

Data acquisition and analysis

Signals were amplified with a Multiclamp 700A amplifier (Axon Instruments, Foster City, CA), low-pass filtered at 20 KHz and sampled at 4 kHz. A Digidata 1320 digitizer (Axon Instruments, Foster City, CA) and PClamp9 (Axon Instruments) were used for data acquisition. Locally written software (J. R. Huguenard, Stanford University School of Medicine) were used to detect (WDETECTA, a postsynaptic current detection program), sort and isolate (WINSCANSELECT) spontaneous EPSCs. Data were then analyzed with PCLAMP9 (Axon instruments) and ORIGIN (Microcal Software, Northampton, MA). The amplitude and kinetics of isolated spontaneous EPSCS (∼20% of of total sEPSCs were well isolated in any given recording; range 8–51% and 12–29% in heterozygous and homozygous *Gria4*^{spwk1} mice, respectively) were used for quantification and analysis. Results are presented as mean ± sem. Data obtained in homozygous versus heterozygous *Gria4*^{spwk1} mice were statistically compared by using the Student's *t*-test. Differences were considered significant if $P < 0.05$.

Miniature (i.e. action potential independent) synaptic events reflect the responses to spontaneously released single vesicles, and therefore provide a readily accessible means to quantify quantal events. The spontaneous EPSCs we recorded here might have been contaminated by action potential-dependent events potentially reflecting multivesicular release. While such multivesicular events could conceivably activate a different set of receptors than those activated by quantal release, we recorded as well EPSCs during the blockade of activity (action potential) via 1 μM tetrodotoxin (TTX, Tocris), a Na^+ channel blocker. Under these conditions, the amplitude, kinetics or frequency of sEPSCs are not affected, indicating that in the mouse thalamic reticular nucleus, the great majority, if not all of the spontaneously occurring events, were in fact miniature events. Also, multivesicular synaptic release is not a significant concern for this study. In rat thalamic reticular nucleus, it has also been shown that spontaneous inhibitory synaptic activity appears to be mainly composed of miniature events (51).

Accession numbers

The DNA sequence of the IAP insertion in *Gria4* is GenBank accession no. EU529742. The DNA sequence of the deletion in the *Gria4*^{tm1Dgen} allele is GenBank accession no. EU529743.

ACKNOWLEDGEMENTS

We thank Emily Patek and Carolyne Dunbar for technical assistance, Kathy Mohr of the University of North Carolina for facilitating the importation of *Gria3* and *Gria4* mutant mice, Dr Julia Brill for assistance with tissue microdissection and Drs Greg Cox, Rob Burgess and Zhong-wei Zhang for helpful discussions and comments. Funding to pay the open access publication charges for this article was provided by the National Institutes of Health.

Conflict of Interest statement. None declared.

FUNDING

This work was supported by NIH grant NS31348 to W.N.F., NS32801 to V.A.L. and NS34744 to J.R.H. The Jackson Laboratory's Cryopreservation, Gene Expression and DNA Sequencing services were subsidized by an NCI core grant CA34196.

REFERENCES

1. Wyllie, E. (1993) *The Treatment of Epilepsy: Principles and Practice*. Lea & Febiger, Philadelphia.
2. McCormick, D.A. and Contreras, D. (2001) On the cellular and network bases of epileptic seizures. *Annu. Rev. Physiol.*, **63**, 815–846.
3. Avanzini, G., Vergnes, M., Spreafico, R. and Marescaux, C. (1993) Calcium-dependent regulation of genetically determined spike and waves by the reticular thalamic nucleus of rats. *Epilepsia*, **34**, 1–7.
4. Jones, E.G. (2002) Thalamic circuitry and thalamocortical synchrony. *Philos. Trans. R. Soc. Lond. B. Biol. Sci.*, **357**, 1659–1673.
5. Berkovic, S.F., Howell, R.A., Hay, D.A. and Hopper, J.L. (1998) Epilepsies in twins: genetics of the major epilepsy syndromes. *Ann. Neurol.*, **43**, 435–445.
6. Khosravani, H. and Zamponi, G.W. (2006) Voltage-gated calcium channels and idiopathic generalized epilepsies. *Physiol. Rev.*, **86**, 941–966.
7. Ludwig, A., Budde, T., Stieber, J., Moosmang, S., Wahl, C., Holthoff, K., Langebartels, A., Wotjak, C., Munsch, T., Zong, X. *et al.* (2003) Absence epilepsy and sinus dysrhythmia in mice lacking the pacemaker channel HCN2. *EMBO J.*, **22**, 216–224.
8. Kim, D., Song, I., Keum, S., Lee, T., Jeong, M.J., Kim, S.S., McEnery, M.W. and Shin, H.S. (2001) Lack of the burst firing of thalamocortical relay neurons and resistance to absence seizures in mice lacking $alpha_{1G}$ T-type Ca^{2+} channels. *Neuron*, **31**, 35–45.
9. Barclay, J., Balaguero, N., Mione, M., Ackerman, S.L., Letts, V.A., Brodbeck, J., Canti, C., Meir, A., Page, K.M., Kusumi, K. *et al.* (2001) Ducky mouse phenotype of epilepsy and ataxia is associated with mutations in the *Cacna2d2* gene and decreased calcium channel current in cerebellar Purkinje cells. *J. Neurosci.*, **21**, 6095–6104.
10. Burgess, D.L., Jones, J.M., Meisler, M.H. and Noebels, J.L. (1997) Mutation of the Ca^{2+} channel β subunit gene *Cchb4* is associated with ataxia and seizures in the lethargic (*lh*) mouse. *Cell*, **88**, 385–392.
11. Fletcher, C.F., Lutz, C.M., O'Sullivan, T.N., Shaughnessy, J.D., Jr, Hawkes, R., Frankel, W.N., Copeland, N.G. and Jenkins, N.A. (1996) Absence epilepsy in tottering mutant mice is associated with calcium channel defects. *Cell*, **87**, 607–617.
12. Letts, V.A., Felix, R., Biddlecome, G.H., Arikkath, J., Mahaffey, C.L., Valenzuela, A., Bartlett, F.S., II, Mori, Y., Campbell, K.P. and Frankel, W.N. (1998) The mouse stargazer gene encodes a neuronal Ca2+ channel γ subunit. *Nat. Genet.*, **19**, 340–347.
13. Zhang, Y., Mori, M., Burgess, D.L. and Noebels, J.L. (2002) Mutations in high-voltage-activated calcium channel genes stimulate low-voltage-activated currents in mouse thalamic relay neurons. *J. Neurosci.*, **22**, 6362–6371.
14. Song, I., Kim, D., Choi, S., Sun, M., Kim, Y. and Shin, H.S. (2004) Role of the alpha1G T-type calcium channel in spontaneous absence seizures in mutant mice. *J. Neurosci.*, **24**, 5249–5257.
15. Huntsman, M.M., Porcello, D.M., Homanics, G.E., DeLorey, T.M. and Huguenard, J.R. (1999) Reciprocal inhibitory connections and network synchrony in the mammalian thalamus. *Science*, **283**, 541–543.
16. Klein, J.P., Khera, D.S., Nersesyan, H., Kimchi, E.Y., Waxman, S.G. and Blumenfeld, H. (2004) Dysregulation of sodium channel expression in cortical neurons in a rodent model of absence epilepsy. *Brain Res.*, **1000**, 102–109.
17. Gauguier, D., van Luijtelaar, G., Bihoreau, M.T., Wilder, S.P., Godfrey, R.F., Vossen, J., Coenen, A. and Cox, R.D. (2004) Chromosomal mapping of genetic loci controlling absence epilepsy phenotypes in the WAG/Rij rat. *Epilepsia*, **45**, 908–915.
18. Rudolf, G., Bihoreau, M.T., Godfrey, R.F., Wilder, S.P., Cox, R.D., Lathrop, M., Marescaux, C. and Gauguier, D. (2004) Polygenic control of idiopathic generalized epilepsy phenotypes in the genetic absence rats from Strasbourg (GAERS). *Epilepsia*, **45**, 301–308.
19. Ozawa, S., Kamiya, H. and Tsuzuki, K. (1998) Glutamate receptors in the mammalian central nervous system. *Prog. Neurobiol.*, **54**, 581–618.
20. Nowak, L., Bregestovski, P., Ascher, P., Herbet, A. and Prochiantz, A. (1984) Magnesium gates glutamate-activated channels in mouse central neurones. *Nature*, **307**, 462–465.
21. Mineff, E.M. and Weinberg, R.J. (2000) Differential synaptic distribution of AMPA receptor subunits in the ventral posterior and reticular thalamic nuclei of the rat. *Neurosci.*, **101**, 969–982.
22. Keinanen, K., Wisden, W., Sommer, B., Werner, P., Herb, A., Verdoorn, T.A., Sakmann, B. and Seeburg, P.H. (1990) A family of AMPA-selective glutamate receptors. *Science*, **249**, 556–560.
23. Petralia, R.S. and Wenthold, R.J. (1992) Light and electron immunocytochemical localization of AMPA-selective glutamate receptors in the rat brain. *J. Comp. Neurol.*, **318**, 329–354.
24. Sato, K., Kiyama, H., Park, H.T. and Tohyama, M. (1993) AMPA, KA and NMDA receptors are expressed in the rat DRG neurones. *Neuroreport*, **4**, 1263–1265.
25. Geiger, J.R., Melcher, T., Koh, D.S., Sakmann, B., Seeburg, P.H., Jonas, P. and Monyer, H. (1995) Relative abundance of subunit mRNAs determines gating and Ca2+ permeability of AMPA receptors in principal neurons and interneurons in rat CNS. *Neuron*, **15**, 193–204.
26. Mosbacher, J., Schoepfer, R., Monyer, H., Burnashev, N., Seeburg, P.H. and Ruppersberg, J.P. (1994) A molecular determinant for submillisecond desensitization in glutamate receptors. *Science*, **266**, 1059–1062.
27. Meeren, H.K., Pijn, J.P., Van Luijtelaar, E.L., Coenen, A.M. and Lopes da Silva, F.H. (2002) Cortical focus drives widespread corticothalamic networks during spontaneous absence seizures in rats. *J. Neurosci.*, **22**, 1480–1495.
28. Bal, T., Debay, D. and Destexhe, A. (2000) Cortical feedback controls the frequency and synchrony of oscillations in the visual thalamus. *J. Neurosci.*, **20**, 7478–7488.
29. Blumenfeld, H. and McCormick, D.A. (2000) Corticothalamic inputs control the pattern of activity generated in thalamocortical networks. *J. Neurosci.*, **20**, 5153–5162.
30. Bowes, C., Li, T., Danciger, M., Baxter, L.C., Applebury, M.L. and Farber, D.B. (1990) Retinal degeneration in the rd mouse is caused by a defect in the beta subunit of rod cGMP-phosphodiesterase. *Nature*, **347**, 677–680.
31. Poltorak, A., He, X., Smirnova, I., Liu, M.Y., Van Huffel, C., Du, X., Birdwell, D., Alejos, E., Silva, M., Galanos, C. *et al.* (1998) Defective LPS signaling in C3H/HeJ and C57BL/10ScCr mice: mutations in Tlr4 gene. *Science*, **282**, 2085–20888.
32. Frankel, W.N., Beyer, B., Maxwell, C.R., Pretel, S., Letts, V.A. and Siegel, S.J. (2005) Development of a new genetic model for absence epilepsy: spike-wave seizures in C3H/He and backcross mice. *J. Neurosci.*, **25**, 3452–3458.
33. Ryan, L.J. and Sharpless, S.K. (1979) Genetically determined spontaneous and pentylenetetrazol-induced brief spindle episodes in mice. *Exp. Neurol.*, **66**, 493–508.
34. Veatch, L.M. and Becker, H.C. (2002) Electrographic and behavioral indices of ethanol withdrawal sensitization. *Brain. Res.*, **946**, 272–282.
35. Maksakova, I.A., Romanish, M.T., Gagnier, L., Dunn, C.A., van de Lagemaat, L.N. and Mager, D.L. (2006) Retroviral elements and their hosts: insertional mutagenesis in the mouse germ line. *PLoS Genet.*, **2**, e2.
36. Golshani, P., Liu, X.B. and Jones, E.G. (2001) Differences in quantal amplitude reflect GluR4- subunit number at corticothalamic synapses on two populations of thalamic neurons. *Proc. Natl Acad. Sci. USA*, **98**, 4172–41777.

37. Hollmann, M. and Heinemann, S. (1994) Cloned glutamate receptors. *Annu. Rev. Neurosci.*, **17**, 31–108.
38. Huguenard, J.R. and McCormick, D.A. (2007) Thalamic synchrony and dynamic regulation of global forebrain oscillations. *Trends Neurosci.*, **30**, 350–356.
39. Liu, Z., Vergnes, M., Depaulis, A. and Marescaux, C. (1991) Evidence for a critical role of GABAergic transmission within the thalamus in the genesis and control of absence seizures in the rat. *Brain Res.*, **545**, 1–7.
40. Liu, Z., Vergnes, M., Depaulis, A. and Marescaux, C. (1992) Involvement of intrathalamic GABAB neurotransmission in the control of absence seizures in the rat. *Neuroscience*, **48**, 87–93.
41. Sohal, V.S., Huntsman, M.M. and Huguenard, J.R. (2000) Reciprocal inhibitory connections regulate the spatiotemporal properties of intrathalamic oscillations. *J. Neurosci.*, **20**, 1735–1745.
42. Meeren, H., van Luijtelaar, G., Lopes da Silva, F. and Coenen, A. (2005) Evolving concepts on the pathophysiology of absence seizures: the cortical focus theory. *Arch. Neurol.*, **62**, 371–376.
43. Khan, Z., Carey, J., Park, H.J., Lehar, M., Lasker, D. and Jinnah, H.A. (2004) Abnormal motor behavior and vestibular dysfunction in the stargazer mouse mutant. *Neuroscience*, **127**, 785–796.
44. Noebels, J.L., Qiao, X., Bronson, R.T., Spencer, C. and Davisson, M.T. (1990) Stargazer: a new neurological mutant on Chromosome 15 in the mouse with prolonged cortical seizures. *Epilepsy Res.*, **7**, 129–135.
45. Hosford, D.A., Clark, S., Cao, Z., Wilson, W.A., Jr, Lin, F.H., Morrisett, R.A. and Huin, A. (1992) The role of $GABA_B$ receptor activation in absence seizures of lethargic (lh/lh) mice. *Science*, **257**, 398–401.
46. Noebels, J.L. and Sidman, R.L. (1979) Inherited epilepsy: Spike-wave and focal motor seizures in the mutant mouse tottering. *Science*, **204**, 1334–1336.
47. Chen, L., Chetkovich, D.M., Petralia, R.S., Sweeney, N.T., Kawasaki, Y., Wenthold, R.J., Bredt, D.S. and Nicoll, R.A. (2000) Stargazing regulates synaptic targeting of AMPA receptors by two distinct mechanisms. *Nature*, **408**, 936–943.
48. Tomita, S., Shenoy, A., Fukata, Y., Nicoll, R.A. and Bredt, D.S. (2007) Stargazin interacts functionally with the AMPA receptor glutamate-binding module. *Neuropharm.*, **52**, 87–91.
49. Malinow, R. and Malenka, R.C. (2002) AMPA receptor trafficking and synaptic plasticity. *Annu. Rev. Neurosci.*, **25**, 103–126.
50. Wu, H., Kerr, M.K., Cui, X. and Churchill, G.A. (2003) A software package for the analysis of spotted cDNA microarray experiments. In Parmigiani, G., Garret, E.S., Irizarry, R.A. and Zeger, S.L. (eds), *The Analysis of Gene Expression Data: an Overview of Methods and Software*. Springer, New York.
51. Huntsman, M.M. and Huguenard, J.R. (2006) Fast IPSCs in rat thalamic reticular nucleus require the GABAA receptor beta1 subunit. *J. Physiol.*, **572**, 459–475.